VELOCITY ANISOTROPY STUDIES

OF

[illegible] FORMATIONS

By

Donald W. [illegible]rritt

A THESIS

Submitted to
Michigan State University
in partial fulfillment of the requirements
for the degree of

MASTER OF SCIENCE

Department of Geology

1961

G 18557
11/23/61

ACKNOWLEDGMENTS

The author wishes to express his sincere appreciation to:

The Cleveland Cliff Iron Company for the use of their seismic refraction equipment with associated supplies which were so generously offered, and especially to Mr. Richard Randolph for technical assistance and advice.

The Jones and Loughlin Steel Corporation for transportation facilities and especially Mr. Jack [illegible], [illegible] Geologist, for [illegible] drill-hole information.

Dr. [illegible], [illegible] whose guidance the study was undertaken.

Dr. Harold I. Stonehouse, Dr. James Trow and Dr. Justin Zinn of the Geology Department, Michigan State Universtiy, for their suggestions and criticisms of the manuscript.

Mr. Jack Janssen, Mr. Donald McCarthy and Mr. William Gill, for their assistance in the field.

CONTENTS

INDEX OF TABLES

Page

INDEX OF FIGURES

ABSTRACT

The phenomenon of compressional seismic wave velocity anisotropy in lineated formations was investigated in the field and a search of geophysical literature related to velocity anisotropy was made. Results of shallow seismic refraction surveys in seven different localities on Precambrian metasedimentary and metaigneous rocks comprising eight different lithologies show velocity anisotropy is measurable in the field. Dipping formations which exhibited bedding, jointing, cleavage, or fracturing always had a faster velocity in the directions parallel to the lineation as opposed to velocities perpendicular to the lineation by as much as 53%.

INTRODUCTION

A shallow seismic refraction survey was conducted during the summer of 19[illegible] to study the velocity anisotropy exhibited by selected Precambrian metasedimentary and metaigneous rocks. Adequately sized steeply dipping outcrops and availability of drill-hole information in drift covered areas were the major reasons for selecting the Upper Peninsula of Michigan for this study. The primary objective of this study of velocity anisotropy was to explore the possibility of using this phenomenon as a method for delineating the strike of steeply dipping buried formations which exhibit some degree of lamellar orientation. Secondary objectives were to investigate the range of velocity anisotropy in certain rocks with the purpose of using this information as a criterion not only for identifying steeply dipping banded formations, but also for determining if the subsurface formations exhibit banding. Some of the lithologies studied were: banded iron formations, greenstone, granite gneiss, slate and garnetiferous biotite amphibolite schist.

Many factors contribute to the control of compressional seismic wave velocities through elastic media. One such factor is the effect of banding as determined by mathematical theory of elastic wave velocities in laminated media. In addition, laboratory experiments conducted by various authors indicate that mineral composition of the medium, texture (in the sense of the geometrical aspects of the component particles of the rock, including size, shape, and arrangement) and structure (as used in the petrological sense of the larger features of a rock mass, like bedding, flow banding, jointing, cleavage and breccition), combine to produce a distinct velocity anisotropy.

FACTORS CONTROLLING VELOCITY ANISOTROPY IN ROCKS

The passage of a seismic wave through the earth is an elastic phenomenon, therefore a brief discussion of the elastic nature of solids is presented.

ELASTIC THEORY

Deformation caused by tension or compression is the only type of elastic deformation important to this study. For simple tension or compression there are equal and opposite forces acting on opposite ends of a body which increase or decrease its length from an initial value l_0 to a new value l_1 and at the same time decrease or increase the width from W_0 to W_1. If only a change in shape is involved then the longitudinal component of strain can be defined as

$$\epsilon_l = \frac{l_1 - l_0}{l_0} = \frac{\Delta l}{l_0}$$

and the transverse component of strain can be defined as

$$\epsilon_t = \frac{W_1 - W_0}{W_0} = \frac{\Delta W}{W_0}$$

The ratio of transverse strain to longitudinal strain is defined as Poisson's ratio σ,

$$\sigma = \frac{\epsilon_t}{\epsilon_l} .$$

If in the case of simple tension or compression a change in volume is involved, a cube of unit volume after deformation will assume the shape of a parallelepiped of length $1+\epsilon$ when ϵ is the longitudinal strain, and of width or thickness $1-\sigma\epsilon$. This follows from

$$\sigma = \frac{\epsilon_t}{\epsilon} \qquad \text{or} \qquad \epsilon_t = \sigma\epsilon$$

The volume after deformation is

$$V_1 = (1+\epsilon)(1-\sigma\epsilon)(1-\sigma\epsilon) = 1+\epsilon-2\sigma\epsilon \cdots .$$

where the dots represent terms involving ϵ^2 which are neglected since ϵ is very small compared to unity. The change in volume per unit volume becomes

$$\frac{V_1 - V_0}{V_0} = \frac{\epsilon(1-2\sigma)}{1} = \epsilon(1-2\sigma) .$$

Stress-Strain Relations

Stress-strain relations have been determined from experiments which resulted in Hooke's Law, which states that stresses are linear functions of or proportional to all strain components. For the case of homogeneous isotropic bodies Hooke's Law can be stated by using two constants known as Young's modulus and the shear modulus.

Young's modulus is the force per unit area divided by the change in length per unit length or

$$Y = \frac{F/A}{\Delta l/l} , \qquad \text{or} \quad \epsilon_l = \frac{1}{Y} S_m$$

Where Sn denotes the constant stress and Y is the symbol used for Young's modulus and is the constant for simple tension or compression. All other components of stress are zero but for pure tension there are also two transverse components of strain denoted by ϵ_{ty} and ϵ_{tz}. These transverse components are

$$\epsilon_{ty} = -\sigma\epsilon_l = -\frac{\sigma}{Y} S_m$$
$$\epsilon_{tz} = -\sigma\epsilon_l = -\frac{\sigma}{Y} S_m .$$

The negative sign indicates a transverse contraction if there is an extension in the x direction.

The shear modulus or μ is obtained from Poisson's ratio and Young's modulus. The relationship is

$$\mu = \frac{Y}{2(1+\sigma)} .$$

For the case of pure shear, an x-force acting on a surface whose normal points in the Y direction Hooke's law becomes

$$\gamma = \tan\beta = \frac{1}{\mu} S_m$$

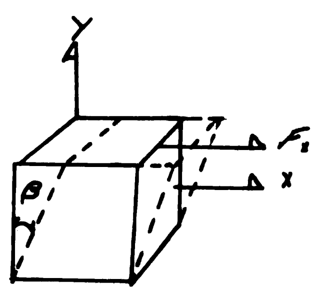

Hooke's Law for Principle Axes

Elastic deformation can be built up as the sum of three simple tensions or compressions along three mutually perpendicular axes known as the principle axes of strain. Similarly the state of stress may be represented by three normal stresses due to tension or compression along three mutually perpendicular axes known as the principle axes of stress. For isotropic bodies these two sets of axes coincide. Denote the principle axis as X_1, X_2 and X_3, then a tension on the X_1 axis produces one component of normal stress S_{x1} and three components of strain ϵ'_{x1}, ϵ'_{x2} and ϵ'_{x3}.

These are related by the equations

$$\epsilon'_{x1} = \frac{1}{Y} S_{x1} \qquad \epsilon'_{x2} = -\frac{\sigma}{Y} S_{x1} \qquad \epsilon'_{x3} = -\frac{\sigma}{Y} S_{x1} ,$$

similarly for the other two axes,

$$\epsilon''_{x1} = -\frac{\sigma}{Y} S_{x2} \qquad \epsilon''_{x2} = \frac{1}{Y} S_{x2} \qquad \epsilon''_{x3} = -\frac{\sigma}{Y} S_{x2}$$

$$\epsilon'''_{x1} = -\frac{\sigma}{Y} S_{x3} \qquad \epsilon'''_{x2} = -\frac{\sigma}{Y} S_{x3} \qquad \epsilon'''_{x3} = \frac{1}{Y} S_{x3} .$$

The resulting strain due to all three tensions or compressions,

S_{x1}, S_{x2}, and S_{x3},

is obtained by simply adding the strain separately produced by each tension. The resulting components of strain are:

$$\epsilon_{x1} = \frac{1}{Y} \left[S_{x1} - \sigma (S_{x2} + S_{x3}) \right]$$

$$\epsilon_{x2} = \frac{1}{Y} \left[S_{x2} - \sigma (S_{x1} + S_{x3}) \right]$$

$$\epsilon_{x3} = \frac{1}{Y} \left[S_{x3} - \sigma (S_{x1} + S_{x2}) \right]$$

also the shear components may be expressed as

$$\frac{\partial \epsilon_{x2}}{\partial x_3} + \frac{\partial \epsilon_{x3}}{\partial x_2} = \frac{2(1+\sigma)}{Y} T_{x1}$$

$$\frac{\partial \epsilon_{x1}}{\partial x_3} + \frac{\partial \epsilon_{x3}}{\partial x_1} = \frac{2(1+\sigma)}{Y} T_{x2}$$

$$\frac{\partial \epsilon_{x1}}{\partial x_2} + \frac{\partial \epsilon_{x2}}{\partial x_1} = \frac{2(1+\sigma)}{Y} T_{x3} .$$

Where τ_{x1} , τ_{x2} and τ_{x3} represent the tangential stresses in the respective directions.

Compositional Banding

The above principles of elastic deformation lead to a theoretical approach to the velocity of elastic waves in laminated media by assuming the material to be in static equilibrium and exposed to certain stresses. These stresses will generate strains similar to those generated by the passage of an elastic wave through the media.

The assumed solid is composed of many layers of laminations whose individual thicknesses are small compared to the wavelengths. This is important because for long wavelengths the average properties control the propagation. When the wavelengths approach the dimensions of the inhomogeneities, the velocity is dependent on the wavelength and attenuation is encountered. It is also assumed that a unit cube containing a fairly large number of layers can be found so that all cubes of this size have the same average properties. This representative cube is still small compared to the wavelength.

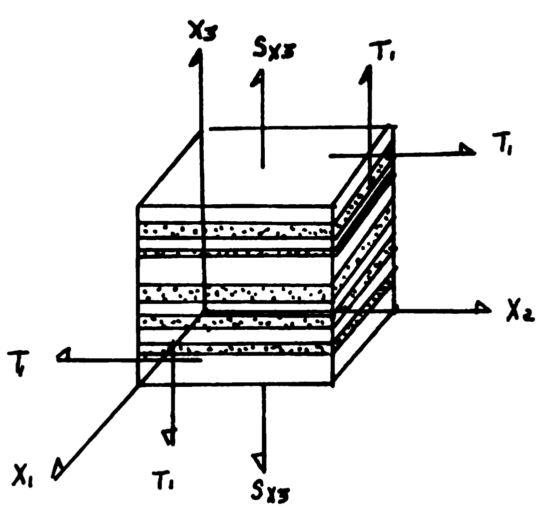

Figure 1. A representative cube in a laminated media.

Vertical Traveling Compressional Waves

The displacements accompanying a plane compressional wave along the x_3 axes are

$$\epsilon_{x1} = 0 \qquad \epsilon_{x2} = 0 \qquad \partial\epsilon_{x3}/\partial x_2 = 0 \qquad \partial\epsilon_{x3}/\partial x_1 = 0$$

The stress-strain relationships in material A of the medium composed of materials A and B are

$$\epsilon_{x1} = \frac{1}{Y}\left[S_{x1} - \sigma(S_{x2} + S_{x3}) \right] = 0$$
$$\epsilon_{x2} = \frac{1}{Y}\left[S_{x2} - \sigma(S_{x1} + S_{x3}) \right] = 0$$
$$\epsilon_{x3} = \frac{1}{Y}\left[S_{x3} - \sigma(S_{x1} + S_{x2}) \right] .$$

Tangential stresses are zero. Elimination of S_{x1} and S_{x2} will give the relationship between stress and strain existing in any layer A. This may be accomplished by adding the equations for ϵ_{x1} and ϵ_{x2}

so $$\frac{S_{x1}}{Y} - \frac{\sigma S_{x1}}{Y} + \frac{S_{x2}}{Y} - \frac{\sigma S_{x2}}{Y} - \frac{2\sigma S_{x3}}{Y} = 0$$

regrouping

$$\frac{1}{Y}\left[S_{x1}(1-\sigma) + S_{x2}(1-\sigma) - 2\sigma S_{x3} = 0\right.$$
$$\frac{1}{Y}\left[(S_{x1} + S_{x2})(1-\sigma) - 2\sigma S_{x3} \right] = 0$$
$$S_{x1} + S_{x2} = 2\sigma S_{x3}/1-\sigma .$$

Substitution of this value of S_{x1} and S_{x2} in the equation for ϵ_{x3} produces

$$\epsilon_{x3} = \frac{1}{Y}\left[S_3 - \sigma\left(\frac{2\sigma S_{x3}}{1-\sigma}\right)\right]$$

which reduces to the formula

$$\epsilon_{x3} = \frac{1}{} \quad \frac{S_{x3}}{(1-\sigma)/1-\sigma-2\sigma^2} = \frac{S_{x3}}{\rho C_A^2}$$

where C_A is the velocity of compressional waves in A and ρ is the density. The change in thickness of a layer is the above strain multiplied by the total thickness of material A, independent of the way in which it is divided into layers. Similar steps can be applied to layer B.

The average strain in the cube is the change in thickness of material A plus the change in thickness of material B divided by the cube dimensions. By designating the portion of the cube composed of material A as n_A and a corresponding meaning for n_B the average stress-strain relationship may be represented by

$$\varepsilon_{x3} = \left(\frac{n_A}{\rho_A C_A^2} + \frac{n_B}{\rho_B C_B^2}\right) S_{x3} \quad .$$

The total density can be expressed as

$$\rho = (n_A \rho_A + n_B \rho_B) \quad .$$

Since the cube moves essentially as a unit, all layers undergo the same acceleration, and the effective density is the total mass divided by the total volume. The effective elastic constant and the effective density yield the expression for propagation velocity

$$\varepsilon_{x3} = \left(n_A/\rho_A C_A^2 + n_B/\rho_B C_B^2 \right) S_{x3} = S_{x3} \; \rho C^2$$

$$C = \left[\frac{1}{\left(\frac{n_A}{\rho_A C_A^2} + \frac{n_B}{\rho_B C_B^2} \right)\left(n_A \rho_A + n_B \rho_B \right)} \right]^{1/2} .$$

Horizontally Traveling Compressional Waves

A compressional wave along X_2 causes a displacement which is uniform in any plane perpendicular to X_2. Hence

$$\partial \varepsilon_{x2} / \partial x_1 = 0 \qquad \partial \varepsilon_{x2} / \partial x_3 = 0 \quad .$$

Shearing stresses are zero, and due to continuity of normal stresses, $S_{x3A} = S_{x3B} = S_{x3}$. ϵ_{x3} can not be zero for the above conditions. The essential requirement is that the thickness of the cube in the X_3 direction does not change. This requirement is maintained if the thickening in material A is accompanied by a thinning in material B as a consequence of the laminated nature of the material. The condition for zero average strain is

$$n_A \, \partial\epsilon_{x3A}/\partial X_3 + n_B \, \partial\epsilon_{x3B}/\partial X_3 = 0 .$$

With these conditions imposed, the stress-strain relations in material A are

$$\epsilon_{x1} = \frac{1}{Y}\left[S_{x1} - \sigma_A(S_{x2} + S_{x3})\right] = 0$$

$$\epsilon_{x2} = \frac{1}{Y}\left[S_{x2} - \sigma_A(S_{x1} + S_{x3})\right]$$

$$\epsilon_{x3} = \frac{1}{Y}\left[S_{x3} - \sigma_A(S_{x1} + S_{x2})\right] .$$

Similar equations apply to material B.

For horizontal travel, the strain ϵ_{x2} is the same in both materials, but the normal stresses S_{x2A} and S_{x2B} are different. By defining an average or effective stress as the total force on the face of the cube divided by the area of that face, the effective stress in terms of the two materials is

$$S_{x2} = n_A S_{x2A} + n_B S_{x2B} .$$

The three stress-strain relations for materials A and B plus the equations for the average strain and the effective stress give a total of eight independent equations from which seven quantities can be eliminated. The quantities

$$S_{x1A},\ S_{x1B},\ S_{x2A},\ S_{x2B},\ S_{x3},\ \partial\epsilon_{x3A}/\partial X_3 \ \&\ \partial\epsilon_{x3B}/\partial X_3$$

were eliminated. The resulting equation gives a constant of proportionality between stresses S_{12} and strain $\partial \epsilon_{x2}/\partial x_2$ which is interpreted as an effective elastic modulus for the laminated material. The effective density is the same as for vertical waves. The square root of the ratio of elastic modulus to density gives the desired velocity for horizontally traveling waves,

$$C = \left[\frac{(n_A^2 + n_B^2) + n_A n_B \left[\frac{2\sigma_A \sigma_B}{(1-\sigma_A)(1-\sigma_B)} + \frac{(1-2\sigma_A)\rho_A C_A^2}{(1-\sigma_A^2)\rho_B C_B^2} + \frac{(1-2\sigma_B)\rho_B C_B^2}{(1-\sigma_B^2)\rho_A C_A^2} \right]}{\left(n_A/\rho_A C_A^2 + n_B/\rho_B C_B^2 \right)\left(n_A \rho_A + n_B \rho_B \right)} \right]^{1/2} .$$

The above derivation is essentially that of J.E. White and F.A. Angona, (1955).

Two graphs are presented which show how the velocity depends upon the physical properties of the individual materials of the laminated material. The velocities are expressed as a ratio of the laminated velocity to the velocity of one of the materials.

For compressional waves traveling in a vertical direction (perpendicular to the bedding), the relationship is shown in Figure 2 page 13 where each curve represents a particular laminated medium. Velocity ratios were varied from 1 to 2 and density ratios from ½ to 2.

For compressional waves traveling in a horizontal direction (parallel to the bending), the expression has a dependence on Poisson's ratio in contrast to the expression for vertical velocities. The results are shown in Figure 3 page 14 where the velocity ratio is plotted as a function of the fractional material of A. Poisson's ratio was given a value of ¼ for both media (Jaeger, 1956).

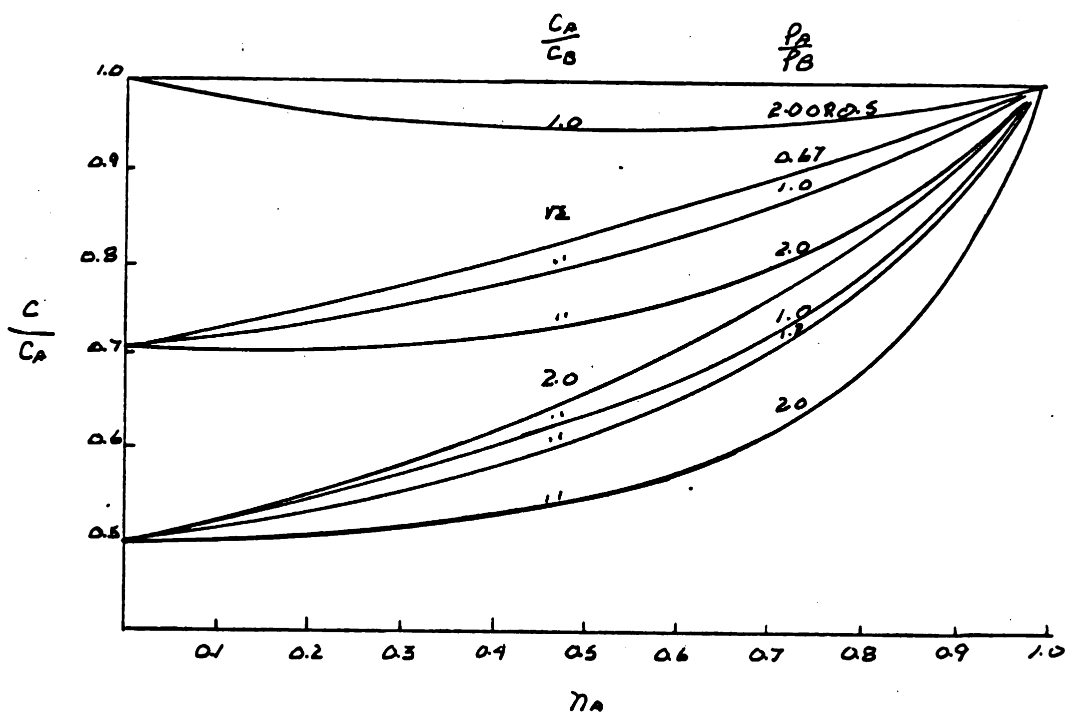

Figure 2

The compressional wave velocity for waves traveling in the vertical direction is plotted against the fraction of material A. Also shown is the effect of changing the density ratio between material A and material B while holding the velocity ratio between them constant.

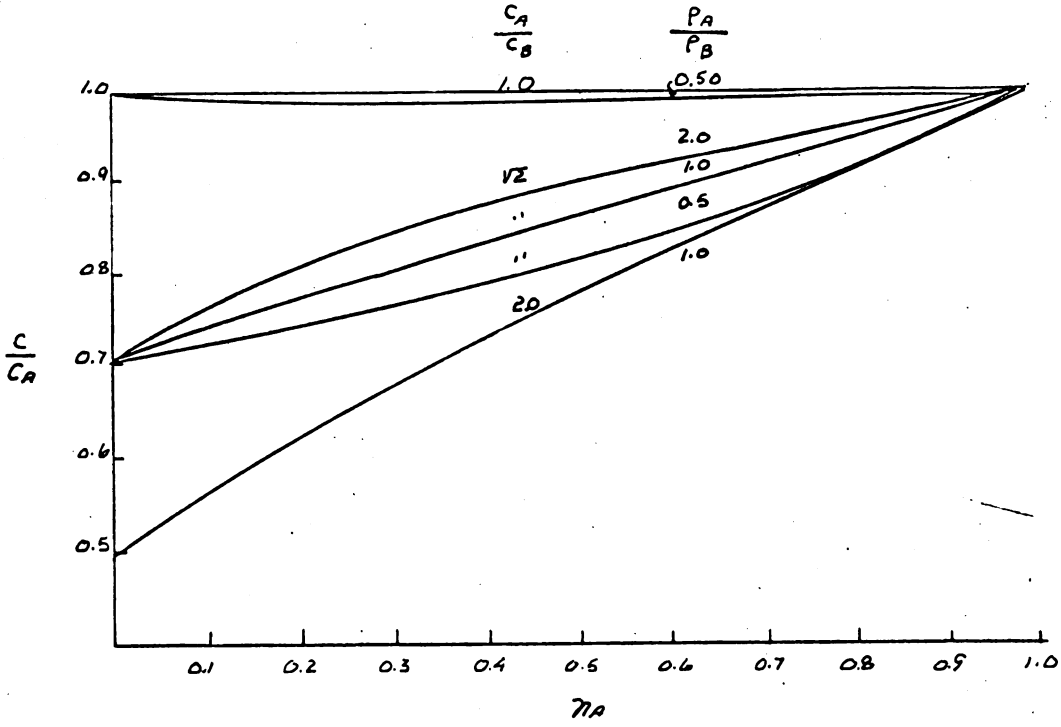

Figure 3

The compressional wave velocity for waves traveling in the horizontal direction is plotted against the fraction of material A. Also shown is the effect of changing the density ratio between material A and material B while holding the velocity ratio between them constant.

The graph for the compressional wave traveling perpendicular to the banding shows that when the velocity ratio between material A and material B is held constant and the density ratio between the two is decreased the ratio between the velocity of material A approaches the velocity of the entire medium. Likewise when the density ratio between material A and material B is held constant and the velocity ratio between the two materials is reduced, the velocity of material A approaches the velocity of the entire medium. The graph for the compressional wave traveling parallel to the banding gives similar results. Where the difference lies is that for any given set of constant conditions the velocity ratio of C/C_A for parallel traveling waves is higher than the same velocity ratio for waves traveling in the horizontal direction. A numerical example may clarify the above statement. Assume the following conditions for waves traveling in both directions

$$C_A/C_B = 2 \qquad \rho_A/\rho_B = 1 \qquad n_A = .5 \;,$$

then from the graph $C/C_A = .63$ for waves traveling perpendicular to the banding and $C/C_A = .77$ for waves traveling parallel to the banding. Let C_A equal 100 fps. Then the average velocity for the entire medium C will equal

$$C/C_A\Big|_{C_A=100} = .63 \qquad C = 63 \text{ F.P.S.}$$

$$C/C_A\Big|_{C_A=100} = .77 \qquad C = 77 \text{ F.P.S.}$$

Although mathematical theory shows the effect banding has on creating velocity anisotropy, it must not be assumed it is the only factor. The following laboratory studies have proven that such lamellar features as fracturing and mineral orientation play an important part in seismic velocities.

Fractures and Voids

Laboratory tests conducted by Wyllie, Gregory, and Gardner, (1956) reveal that as porosity increases the velocities decrease. Slightly fractured samples gave appreciably lower velocities than non-fractured samples. The velocity was not totally dependent upon the porosity but to a high degree on the velocity of the rock matrix material with its attendant intercrystalline porosity. The energy appears to follow the path of maximum velocity, thus bypassing many of the fractures by following a path of minimum travel time in the homogenous matrix of the rock. An important part is played by fractures perpendicular to the wave path which cannot be bypassed and will give lower velocities due to the traversing of the slower medium. This is especially true of air filled fractures caused by jointing, cleavage or bedding plane separation.

The factors which must be considered in such a case are the velocity through the fluids filling the voids (gas or liquid), the velocity through the solid rock alone, the acoustic coupling between the fluid and the rock and the geometric structure of the rock.

Mineral Composition

Most crystals show pronounced velocity anisotropy which is dependent on the axis along which the measurements are made. One of the more common minerals is quartz, where the velocity varies from around 17,000 perpendicular to the C crystallographic axis to 21,500 feet per second parallel to the C crystallographic axis. Furthermore, studies conducted by Laughton, (1957) show a noted anisotropy increase with increasing clay content in ocean sediments after they had been subjected to external pressures in the lab with the velocity greater along the bedding planes than across them. This anisotropy in similar laminated sediments occurs under natural conditions as a result of uniaxial compaction. This was readily observed in velocity measurements of sedimentary rocks and schists conducted by Day, Hill, Laughton, and Swallow, (1956) which show the velocity parallel to the bedding is always greater than the velocity perpendicular to it.

INSTRUMENTATION

A conventional Century twelve trace portable refraction seismograph was employed in this investigation. This instrument, which is designed primarily for shallow seismic studies, is well suited to this type of investigation because the entire unit can be easily transported by two men. It consists of the following components: Seismometers which change the vertical component of earth motion caused by an explosion or other artificial disturbance into electrical impulses which are transmitted by means of a cable to a test unit. This unit provides a rapid means for checking continuity in the various connections and signal leakage caused by the grounding of non-insulated connections. This unit also provides a means of eliminating through an AC balance any steady state signals induced into the geophones or cables by high tension power transmission lines. The signal proceeds from the test unit to an amplifying unit where it is made strong enough to cause galvanometer deflection. Tiny mirrors are attached to the meter movement in such a way that light rays are reflected from the mirrors onto photographic paper. At the same time a timing motor with an attached interrupted disc passing an independent light source is also causing light rays every one hundreth of a second to be photographed on the same paper. The end result is a permanent continous record of galvanometer deflections spaced by timing lines.

The time break or shot instant appears on the number six trace, in a make and break form, that is, there is a half cycle kick when the current is applied to the line or cap by the switch and one of opposite polarity when the cap ruptures. The initiation of the second break is the instant at which the seismic wave originates and is therefore used for time calculations when dynamite was used. When the energy source was not dynamite, the times were measured with reference to a given timing line as described under the section on errors. Two typical records are shown in Figure 4 page 21.

Errors Associated with Instrumentation

A micrometer microscipe was used in making all measurements (measuring distances to the enclosing timing lines and trace break) on the records. The horizontal scale on the microscope is divided into 0.04 inch divisions. This 0.04 inches is broken down into one hundred divisions on the associated drum, making possible the reading of distances on the records to 0.0004 inches. Since the time interval measured (0.01 second) covered, on the average, 0.14 inches a reading of a given point on the record could be made to 0.000029 seconds (0.14:0.01::0.0004:x). In each determination it was necessary to measure the distance between the two timing lines and the instant of arrival of energy, as shown in Figure 4 page 21 .

The condition for maximum error in making a pick would be obtained if all three readings (the two timing lines and the trace break) were additive in the same direction, and would therefore be 0.00009 seconds. In many instances the trace break was not sharp enough to make a pick to the above accuracy (Figure 4 trace 5), but from repeated readings of a large number of records it was concluded that the total error in picking the instant of arrival and measuring the three necessary intervals on any one trace did not exceed 0.0002 seconds.

For any one record all picks were measured relative to some timing line. A minimum time of 0.01 seconds before the first break was always chosen for the reference timing line. This precautionary measure insured an error less than 0.02. That is, the minimum time measured on any one record was at least 0.01 seconds, so since the time could be measured by use of the microscope of 0.0002 seconds the percent error had to be less than (.0002/0.01) x 100 percent.

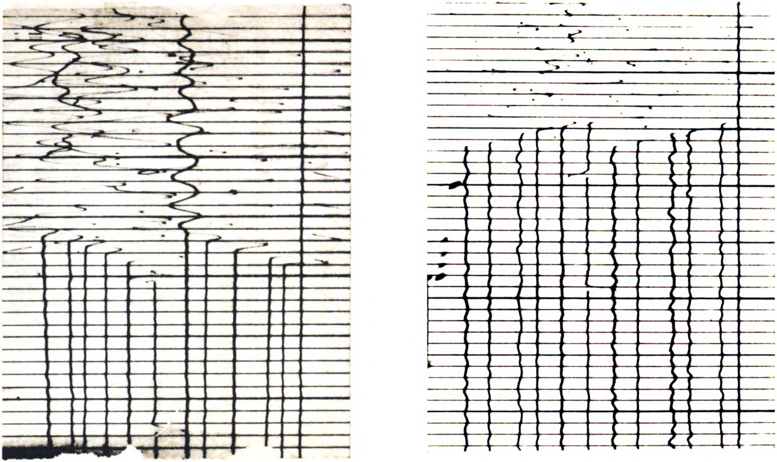

Figure 4

Typical refraction seismograph records

FIELD PROCEDURES

The problem of determining seismic velocity variations with respect to structural orientation dictated that various geophone layouts be used. For any one structural orientation all geophones were placed in a straight line at a constant spaced interval. However, this interval which was carefully measured by steel tape was varied to suit the conditions of the individual areas studied, the shot or energy source was initiated and the record developed. In areas where outcrops were investigated the energy source was sledge hammer blows within a foot of the first geophone. For areas where the refracting horizon was buried, the principle of reciprocity of time was applied. That is, the time required for a wave to travel a given path in one direction would equal the time required for the wave to travel the same path in the opposite direction. In order to apply this principle the dynamite was buried at the end of the normal length of the spread after the first geophone had been moved in half the distance to the second geophone. After the record was taken the same procedure was applied to the opposite end of the spread.

RECORD INTERPRETATION

The plot of time vs. distance provided a rapid and convenient method of analyzing the seismograph records. The slope of all time-distance lines was obtained by the method of least squares.

For records taken on outcrops the velocity is the reciprocal of the slope of the line passing through the origin. For records taken over buried formations, the reciprocal of the slope of the line through the origin gave the velocity of the first horizon V_0 and the reciprocal of the slope of the second line gave the velocity of the second horizon V_1. Where the slope of the second line was not the same when shooting from opposite ends of the geophone spread (Figure 12 graph #1 page 39), the true velocity of the underlying formation was obtained from the following formulas which are derived in any basic geophysics book such as Dobrin, (1952).

$$V_1 = V_0 / \sin i_c$$

$$i_c = \tfrac{1}{2} \left(\sin^{-1} V_0 m_d - \sin^{-1} V_0 m_u \right)$$

m_d is the slope of the down dip segment

m_u is the slope of the up dip segment

These various factors are shown in Figure 5 page 24.

In many instances several duplicate records were made. In each case a least squares curve was determined and the values averaged to enable the presentation of one curve for each locality and shooting orientation. The tabulated results of calculations can be found in Table 1 page 26. Time distance curves are presented in the back.

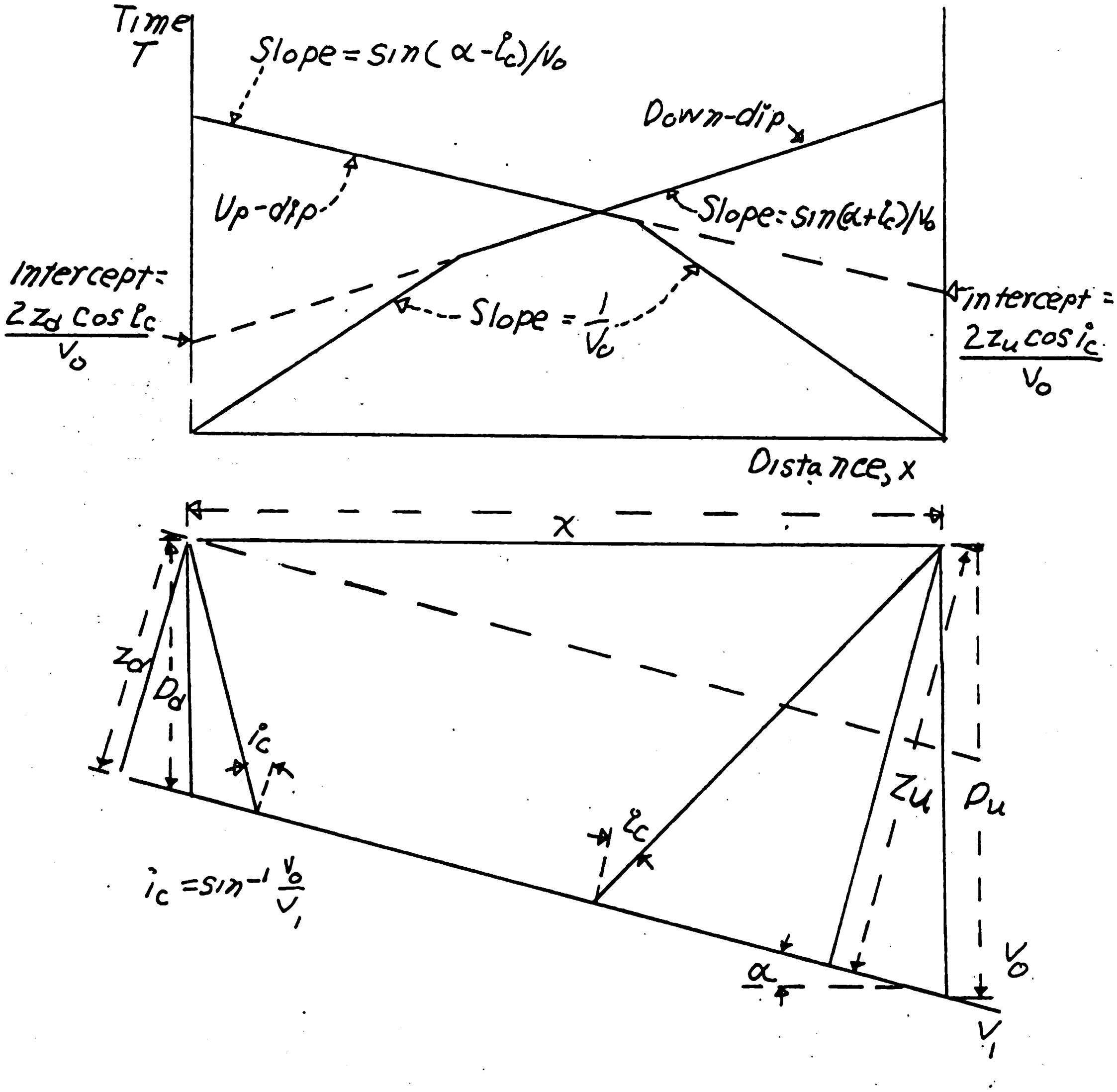

Figure 5

Refraction along an interface dipping at an angle α. Respective shots are at updip and downdip ends of profile.

RESULTS

A total of seven different localities comprising eight different lithologies were studied. All outcrops were lameller either in the form of banding, fracturing, bedding or mineral orientation. They were specifically chosen for these properties. Once it had been established that velocity anisotropy of outcrops was determinable by field investigations, the study was extended to areas covered by glacial till ranging from fifteen to fifty-five feet in depth. Areas of good drill-hole coverage were chosen for these studies since it was necessary to have a check on the results. The tabulated results of these studies are presented in Table 1 page 26.

Area A

The outcrop is composed of two different formations; the Goodrich quartzite and the Negaunee Iron Formation, and is located in the SW¼, sec 16, T46N, R29W, Marquette County, near the town of Republic. The iron formation grades from vertically dipping alternating bands of specular hematite-magnetite and recrystalized chert with minor amounts of epidote, chlorite, magnetite and silicates into a silicate iron formation composed of vertically dipping alternating bands of grunerite and recrystalized chert with minor amounts of magnetite, chlorite, cummingtonite and epidote. Typical banding throughout the entire outcrop is shown in Figure 6 page 27. The chert bands generally range from one-tenth of one-quarter of an inch while those of the iron oxide exhibit considerable variation (micron size to two inches).

TABLE 1

AREA	LITHOLOGY	PARALLEL*	PERPENDICULAR*	DIP	VELOCITY (fps)	VELOCITY RATIO
A	alternating bands of hematite-magnetite and recrystalized chert	X		90°	13,673	.65
			X		9,000	
	alternating bands of grunerite and recrystalized chert	X		90°	17,980	.73
			X		13,200	
	(Negaunee Iron Formation, high metamorphic rank)					
B	banded garnitiferous biotite amphibolite schist, highly contorted	X		90°	7,000	.97
			X		6,800	
C	well banded greenstone schist	X		90°	7,000	.53
	(Mona schist)		X		3,716	
D	peridotite weathering to serpentinite	X		-	13,500	.72
			X		9,690	
E	granite gneiss	X		90°	10,204	.61
			X		6,200	
F	Negaunee Iron Formation (low metamorphic rank)			0°	6,265	.97
					6,092	
G	Siamo slate	X		40°	10,028	
		45°			8,473	.83
			X		7,056	.68

* Direction with respect to lamellar orientation.

Figure 6

#1 Photograph of fractures in Peridotite weathered to Serpentinite in area D.

#2 Photograph of banding displayed in the Negaunee Iron Formation. Area A.

Two lines were run parallel to the banding, one in the specular hematite-magnetite and one in the silicate iron formation. These gave velocities of 13,673 fps and 17,900 fps respectively. An orientation perpendicular to the banding which extended across the entire iron formation was then run with a velocity of 13,200 fps in the silicate iron formation and a velocity of 9,000 fps in the hematite-magnetite.

The time distance curves for the area are shown in Figure 7 page 34. Two or more were taken for each orientation. Geophone spacings of ten and twenty-five feet gave similar velocities.

Area B

A vertically banded garnitiferous biotite amphibolite schist approximately seventy feet long and forty feet wide is located in the SE¼, sec 1, T46N, R30W, Marquette County. This highly contorted schist whose stratigraphic position is either Upper Goodrich, Michigamme, or Greenwood (Villar, unpublished), gave no distinct velocity anisotropy. A ten foot spaced seventy foot long spread parallel to the schistosity resulted in a velocity of 7,000 fps, while a ten foot spaced forty foot long spread perpendicular to the schistosity produced a velocity of 6,900 fps. Duplicate records were taken in both directions. The time distance graphs for this area are shown in Figure 8 page 35.

Area C

This area is located at 46°33' longitude and 87°23' latitude, Marquette County, and is locally known as Lighthouse Point. An approximately vertically dipping section of the Mona schist was studied. The Mona schist at this location is a basic, well banded, greenstone schist. The mineral assemblage is mostly epidote, chlorite, hornblend, plagioclase and quartz (Van Hise, 1911). Geophone orientation parallel to the banding utilizing a ten foot spacing with a spread length of fifty feet produced a velocity of 6,731 fps, while an orientation perpendicular to the banding with a spacing of five feet and a spread length of twenty-five feet produced a velocity of 3,716 fps. The time distance curves are shown in Figure 9 page 36.

Area D

Presque Isle is located north of the City of Marquette at 46°35' longitude and 87°23' latitude. A large flat outcrop of peridotite altered to serpentinite lineated by weathering characteristic as shown in Figure 6 is exposed at the north-east side of the isle. A geophone orientation parallel to the lameller orientation with ten foot spacings and spread length of eighty feet produced a velocity of 13,500 fps, while a similar perpendicular orientation produced a velocity of 9,690 fps. The time distance graphs are shown on page 37, Figure 10.

Area E

Extensive outcrops of granite gneiss are exposed along the road in the NW¼, sec 10, T41N, R30W, Randville Quadrangle Michigan-Wisconsin. The gneissic banding is essentially vertical, and a sixty foot spread length with a ten foot spacing parallel to the banding produced a velocity of 10,204 fps, while a fifty foot spread with a ten foot spacing normal to the banding produced a velocity of 6,800 fps. The time distance graphs are shown in Figure 11 page 38.

Area F

The area is located in the N½ of NE¼ sec 8, T47N, R26W, Marquette

County. Map #1 gives a plan view of the location of the two geophone orientations, and map #2 is a vertical cross section of the area. The drill-hole information reveals fifty-five feet of glacial till overlying horizontal beds of the Negaunee Iron Formation. The geophones were spaced at twenty-five foot intervals with a total spread length of two hundred and fifty feet in both directions. Time distance graphs shown in Figure 12 page 39 give the velocity in the E-W direction as 6,205 fps and in the N-S direction as 6,093 fps.

Area G

This area is located six hundred feet north of area F as shown on map #1. The combination of test pit information and time distance curves on page 40 reveals twelve feet of glacial till directly overlying the Siamo slate which is dipping southward at 40°. Three different geophone orientation were used in an attempt to detect the velocity change with lamellar orientation. The orientations are shown on Map #1 with the first orientation parallel to the strike, the second rotated clockwise through 45° and the third orientation perpendicular to the strike. The time distance graphs on page 40 Figure 13 produce velocities of 10,023 fps, 8,473 fps and 7,056 fps for the respective orientations.

Additional Surveys

A literature search revealed that velocity anisotropy with respect to structure orientation has been observed by other authors. Some of these studies are presented below.

White & Songbush, (1954) while working with shale and loose sand observed that for shale the horizontal compressional velocities obtained were 8,000 fps, the vertical compressional velocities were 6,000 fps, and in loose sand both vertical and horizontal compressional velocity were the same.

Hughes and Cross, (1951) conducting laboratory experiments with argillaceous limestones from well cores, in which "the cores were cut one perpendicular and one parallel to the bedding from very closely neighbring positions. The data shows a definite anisotropy, with the higher velocity parallel to the bedding." Perpendicular to the bedding the velocities at 27°C and 50 bars pressure is 18,733 fps increasing to 20,252 fps at 5,000 bars pressure. For the same conditions, the velocity parallel to the bedding starts at 19,776 fps and increases to 20, 892 fps.

INTERPRETATION OF RESULTS

The results of the field survey provide conclusive evidence that various forms of lineation cause velocity anisotropy. The banding in area A of hematite-magnetite and recrystalized chert along with the banding of grunerite and recrystalized chert produce a distinct velocity anisotropy. The schistosity of the greenstone Mona schist in area C and the slaty cleavage of the buried Siamo slate of area G where the velocity ratio between the orientation at 45° and 90° and the parallel orientation was 7% and 65% respectively, give anisotropic velocity readings. The gneissic texture of the granite gneiss in area D and the fracturing of the serpentinite in area D with the resultant weathering characteristics produce velocity anisotropy. For area B where the schist was highly contorted and no gross lamellar orientation observable, velocity anisotropy was lacking. The absence of a break in the time distance curves for area F where the Negaunee Iron Formation is overlain by fifty-five feet of glacial till may indicate the energy was not being refracted upward or that the formations had similar acoustical properties.

All of the above information gathered from the use of shallow seismic refraction equipment shows that this method can be used to detect velocity anisotropy which in turn may be used for delineating orientation of buried structure.

SUGGESTIONS FOR FURTHER STUDY

This study has shown velocity anisotropy to be detectable in the field. Following, are the recommendations for further study.

Field studies similar to the present study in areas where buried steeply dipping lamellar formations have good drill hole coverage in order to establish the limitations of the method.

Field studies on outcrops to try and correlate the velocity ratio with lithologies, degree of lamellar orientation or differential velocities between the comprising bands.

Laboratory studies on field samples exhibiting various lamellar features to try and determine how much of an effect the individual features may have.

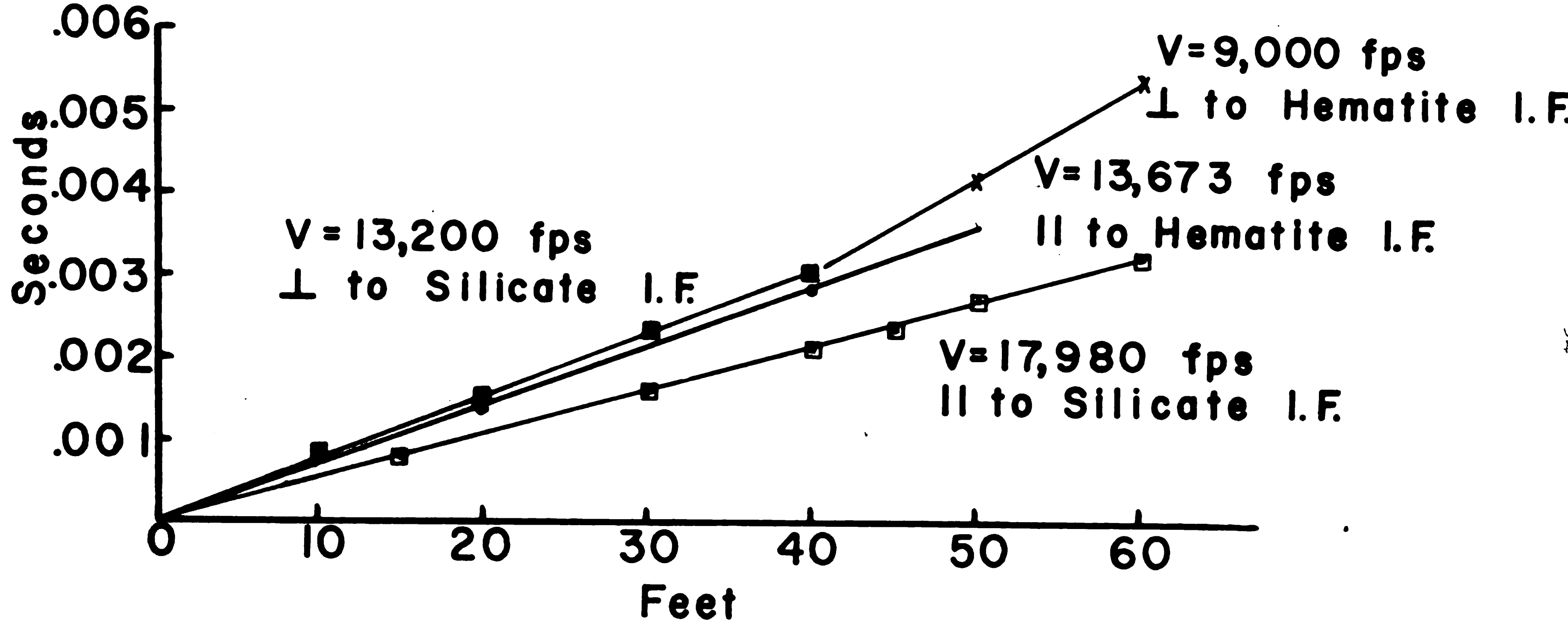

TIME DISTANCE GRAPH FOR AREA A.

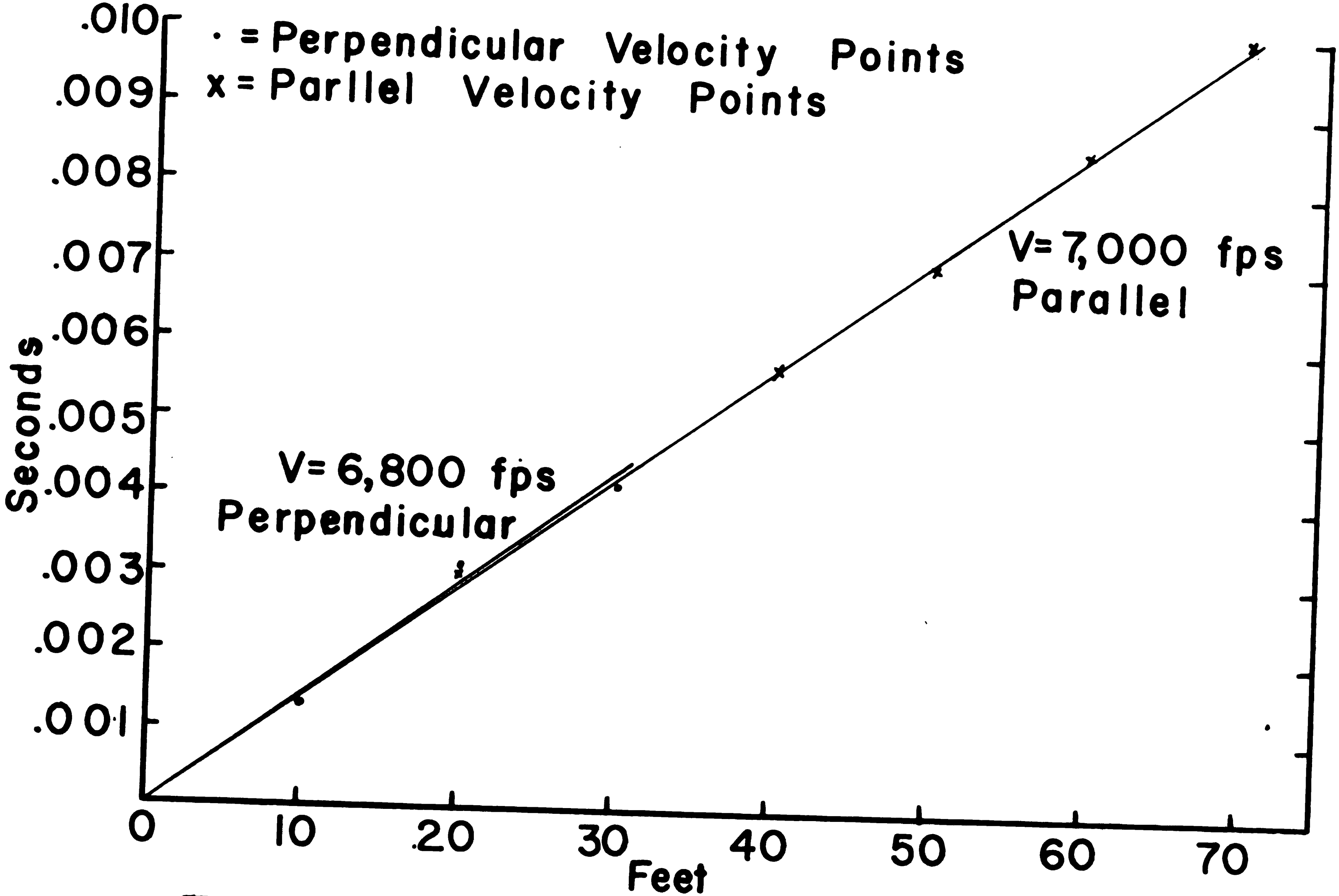

TIME DISTANCE GRAPH FOR AREA B

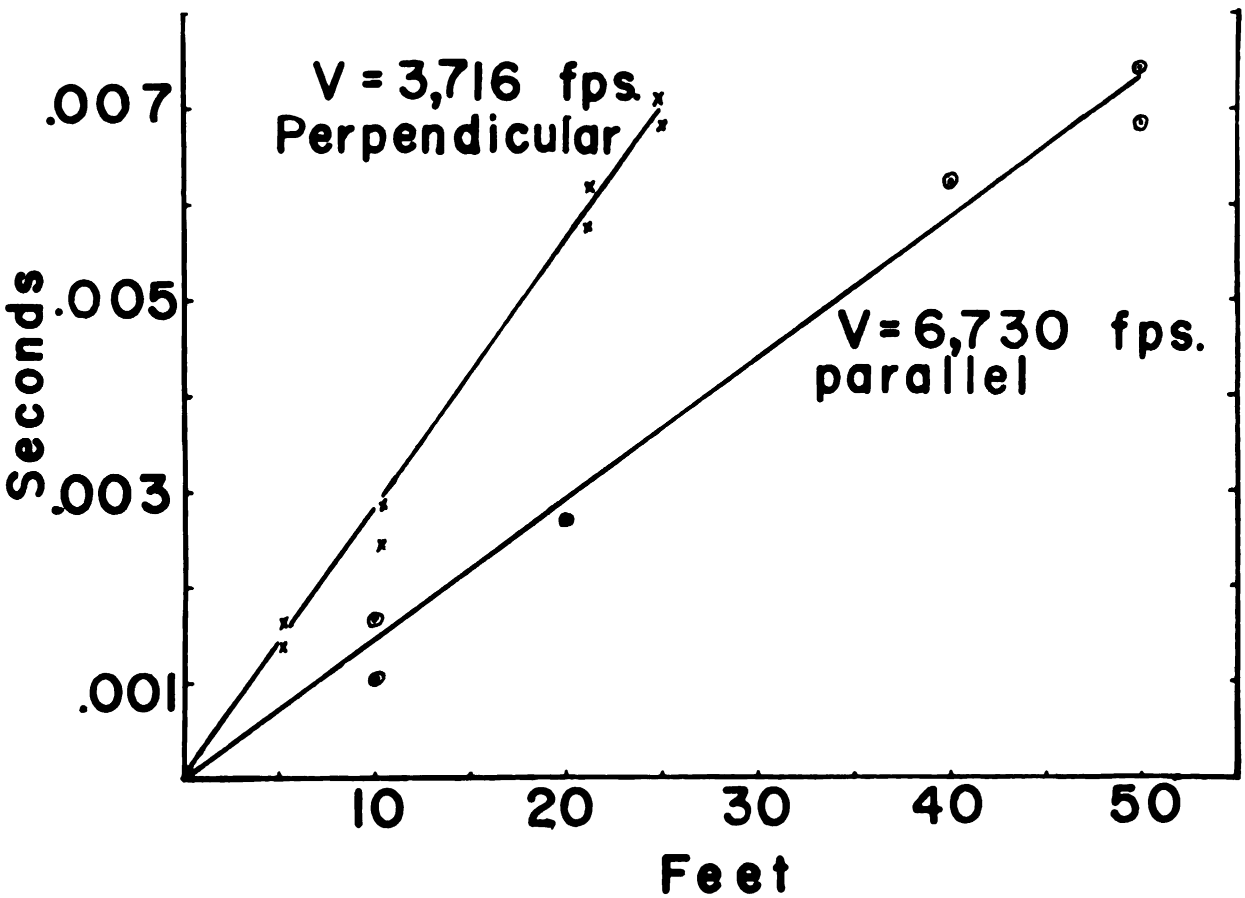

TIME DISTANCE GRAPH AREA C.

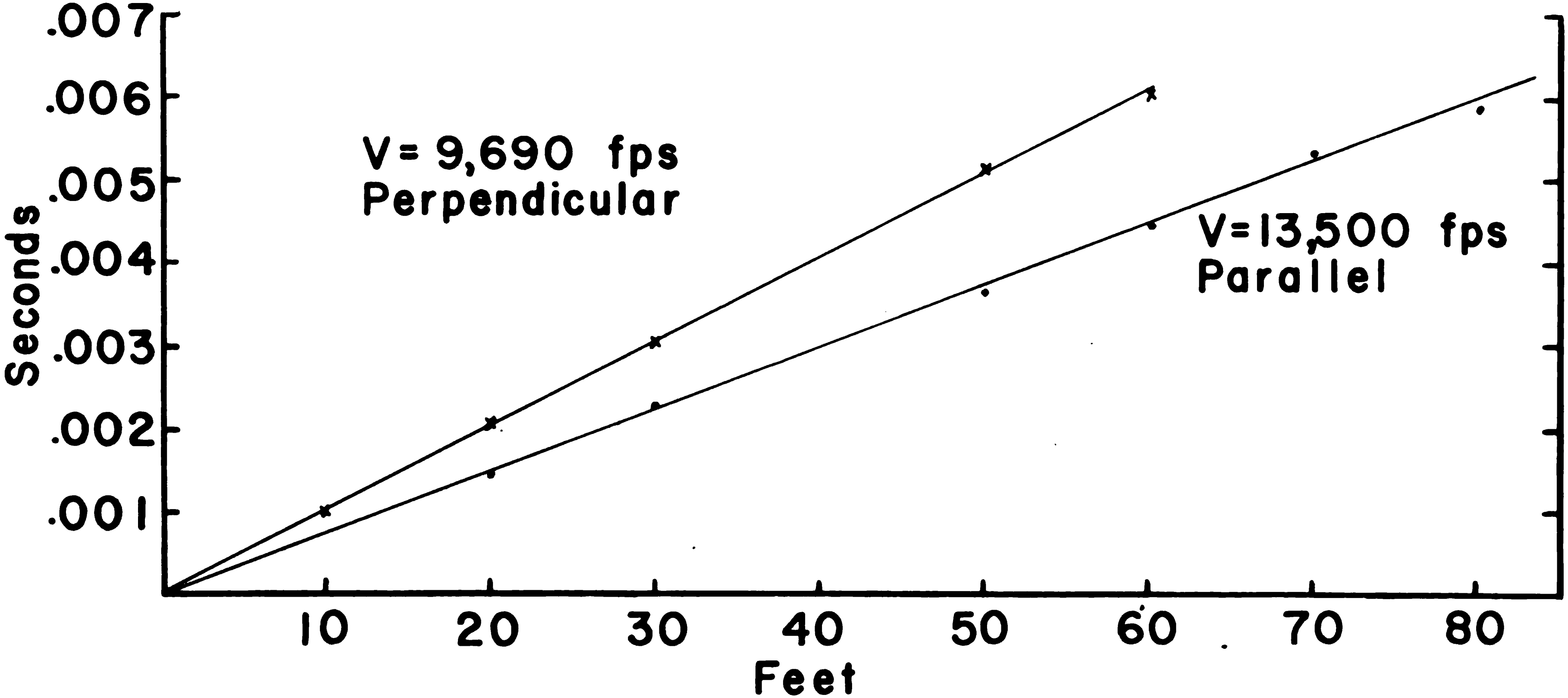

TIME DISTANCE GRAPH FOR AREA D.

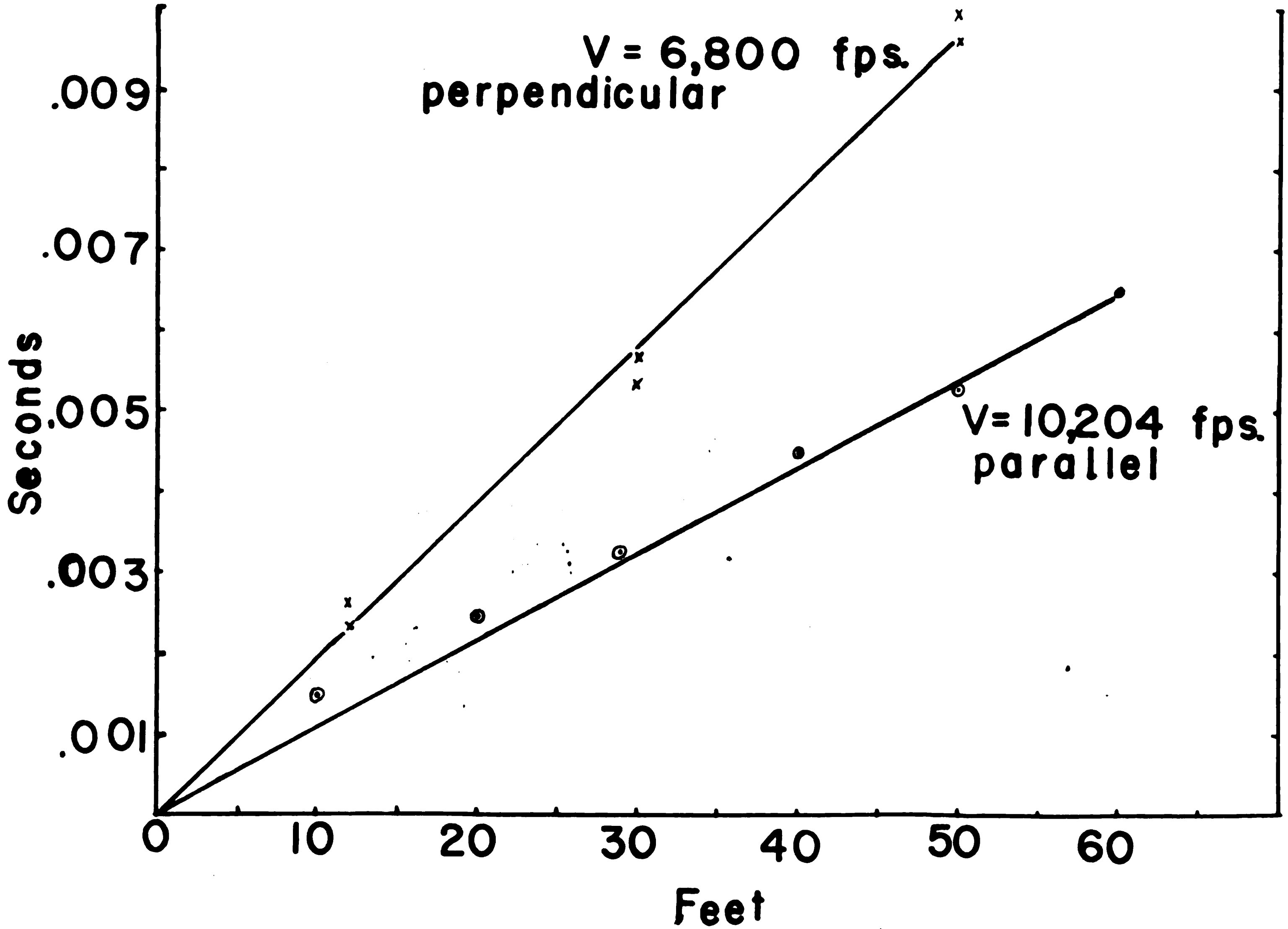

TIME DISTANCE GRAPH AREA E.

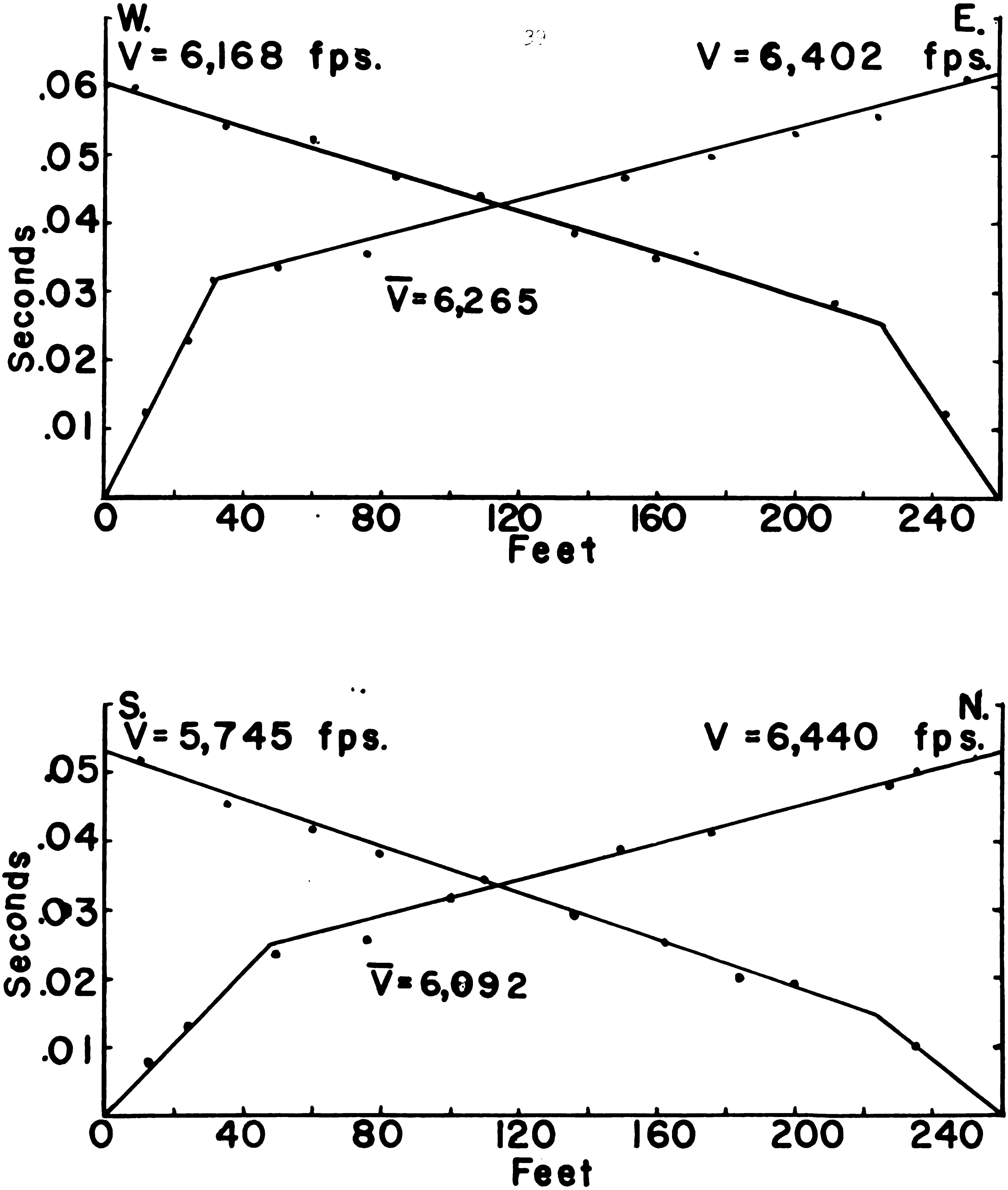

TIME DISTANCE GRAPHS AREA F.

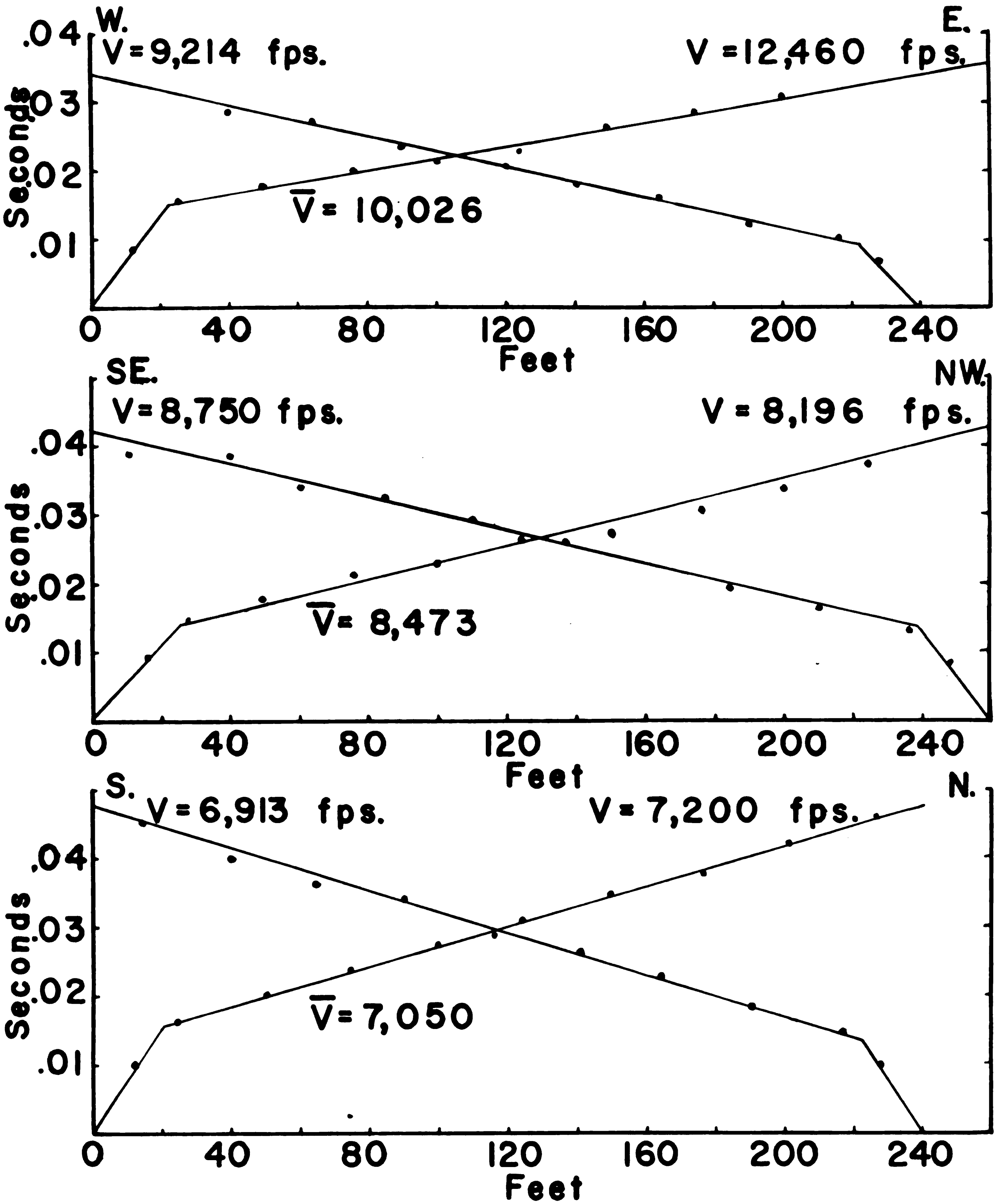

TIME DISTANCE GRAPHS AREA G.

REFERENCES CITED

Dobrin, M.B., 1952, Introduction to geophysical prospecting: New York: McGraw-Hill Book Company, Inc., 435 p.

Hughes, D.S. and Cross, J.H., 1951, Elastic wave velocities in rocks: Geophysics, v. 16, p. 591.

Jaeger, J.C., 1956, Elasticity, fracture and flow: New York: John Wiley and Sons, Inc., p. 58.

Laughton, A.S., 1957, Sound propagation in ocean sediments: Geophysics, v. 22, p. 233-260.

Van Hise, 1911, Geology of the Lake Superior region: U.S. Geological Survey, Monograph 52, p. 254.

Villar, James, Preliminary report of the petrography and petrology of the iron formation near Republic, Michigan: Michigan State University, unpublished.

White and Angona, 1955, Elastic wave velocities in laminated media: The Journal of the Acoustical Society of America, v. 27, p. 310-317.

White, J.D. and Songbush, R.L., 1954, Velocity measurements in near surface formations: Geophysics, v. 16, p. 591.

Wyllie, Gregory and Gardner, 1946, Factors affecting velocity: Geophysics, v. 23, p. 479.

[redacted]

[redacted]

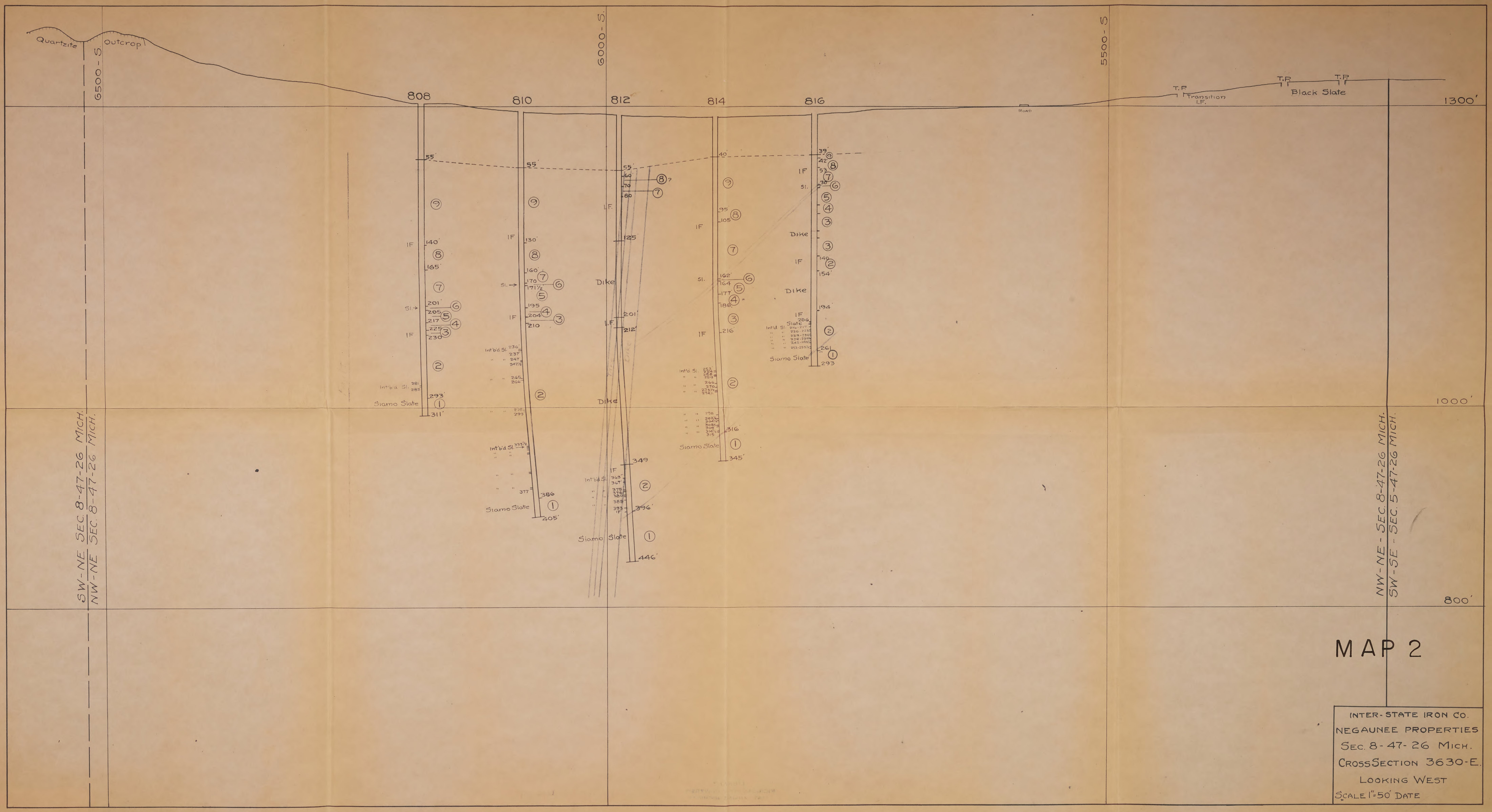

Quartzite Outcrop
6500-S
6000-S
5500-S
808
810
812
814
816
T.P.
Transition I.F.
Black Slate
Road
1300'
1000'
800'
IF
Sl.
Dike
Int'b'd Sl.
Siamo Slate
SW-NE SEC. 8-47-26 MICH.
NW-NE SEC. 8-47-26 MICH.
NW-NE - SEC. 8-47-26 MICH.
SW-SE - SEC. 5-47-26 MICH.
MAP 2
INTER-STATE IRON CO.
NEGAUNEE PROPERTIES
SEC. 8-47-26 MICH.
CROSS SECTION 3630-E.
LOOKING WEST
SCALE 1"=50' DATE

C-18-67

Pocket has: 2 maps